



The impact of a low-permeability upper layer on transient seawater intrusion in coastal aquifers

Antoifi Abdoulhalik^{a,**}, Ashraf Ahmed^{b,*}, Abdelrahman Abdelgawad^c, Gerard Hamill^a

^a School of Natural and Built Environment, Queen's University Belfast, Belfast, BT7 1NN, UK

^b Department of Civil and Environmental Engineering, Brunel University London, Uxbridge, UB83PH, UK

^c Department of Civil Engineering, Faculty of Engineering, Assiut University, Assiut, Egypt

ARTICLE INFO

Keywords:

Saltwater intrusion
Coastal aquifer management
Salinization mitigation
Groundwater flow
SEAWAT
MODFLOW

ABSTRACT

This paper provides a thorough investigation of the effect of a top low-permeability (TLK) layer on transient saltwater intrusion dynamics prompted by water table fluctuations and sea level rise. Laboratory experiments were conducted on a 2D-sandbox and numerical simulations were performed using the SEAWAT code. Four cases were investigated, including a homogeneous case and three cases, where the top layer thickness (W_{top}) was equal to 0.2H, 0.33H and 0.5H, respectively, where H was the aquifer thickness. The experimental and numerical results show that the toe length decreases linearly with increasing the thickness of the TLK layer. The results also suggest that lowering the permeability of the upper part of the aquifer causes faster saltwater removal process. The sensitivity analysis shows that decreasing the top layer permeability causes further reduction of the intrusion length. Nonetheless, the results evidence that this method yields relatively little reduction of the saline water intrusion length if the upper layer thickness is inferior or equal to a fifth of the total aquifer thickness, regardless of the permeability value of the top layer. The field-scale modelling results demonstrate that the performance of the TLK layer weakens noticeably as the hydraulic gradient decreases. The results show that the TLK layer achieved a maximum saltwater wedge reduction of 31% in the case where $W_{top} = 0.75H$, which means that lowering the permeability of three fourths of the aquifer thickness only induced a toe length reduction by nearly a third of its original length. In addition to providing a quantitative analysis of SWI dynamics in bi-layered coastal aquifers, this study questions the performance and practicality of the artificial reduction of the upper aquifer permeability as a countermeasure for seawater intrusion control.

1. Introduction

Saline water intrusion (SWI) is a natural process that led to the contamination of many coastal aquifers around the world. The main metrics quantifying SWI include the saltwater wedge toe length and the width of the freshwater/saltwater interface, which delineate the outer boundary of the saline plume as it encroaches coastal aquifers. The seawater toe length, which represents the distance at which the freshwater-saltwater interface intersects the impermeable bottom of the aquifer, gives a good indication about how deep the saltwater wedge has penetrated the aquifer system. Therefore, accurate prediction of toe length is essential from a water resources management standpoint. The accurate delineation of the interface position may, however, be challenging, given its strong dependency on climate change effects, such as

drought, and sea-level rise.

Many methods were suggested in the literature to control saline intrusion in coastal aquifers. One of these methods is the subsurface dams, which are physical barriers placed at the bottom of the aquifer resting on an impervious layer. Luyun (2009) investigated these barriers for homogeneous aquifers and found them effective. Shorter subsurface dams helped cleaning up the aquifer faster than the taller dams. Using the experimental automated image analysis technique, Abdoulhalik and Ahmed (2017a) demonstrated that subsurface dams were also effective in controlling seawater intrusion for the case of heterogeneous layered aquifers. The presence of low-K layer at the top or the bottom of the aquifer prolonged the cleanup time, up to 50% longer when the lower-K layer was at the bottom, compared to the case of a homogeneous aquifer. The effectiveness of subsurface dams was also investigated by Chang

* Corresponding author.

** Corresponding author.

E-mail addresses: abdoulhalik01@qub.ac.uk (A. Abdoulhalik), ashraf.ahmed@brunel.ac.uk (A. Ahmed).

<https://doi.org/10.1016/j.jenvman.2022.114602>

Received 18 June 2021; Received in revised form 9 December 2021; Accepted 24 January 2022

Available online 29 January 2022

0301-4797/© 2022 Elsevier Ltd. This is an open access article under the CC BY license (<http://creativecommons.org/licenses/by/4.0/>).

et al. (2019).

Abdoulhalik and Ahmed (2017b) evaluated the use of cutoff walls to reduce SWI in heterogeneous aquifers. The presence of an interlayer of low permeability inhibited the downward movement of the freshwater towards the wall opening, and thereby decreased the repulsion ability of the cutoff wall. Also, the presence of an underlying low permeability layer obstructed the freshwater flow in the lower part of the aquifer and hence slowed down the velocity through the wall opening. Abdoulhalik et al. (2017) then suggested a new mixed physical barrier (MPB) system that was found more effective than the traditional barrier systems. The MPB system, with only 40% wall depth, achieved 13% greater reduction in the saltwater wedge toe length than the use of cutoff wall with 90% penetration depth.

Other investigators used the hydraulic barrier system to control saline intrusion. Hydraulic barriers can be either a negative hydraulic barrier (e.g., Pool and Carrera, 2010), where saltwater is abstracted from the aquifer, or positive hydraulic barrier (e.g., Botero-Acosta and Donado, 2015), where freshwater is injected into the aquifer to repulse the saline water wedge, or a combination of both. Armanuos et al. (2019) found the use of a combination of a physical and hydraulic barrier is very effective in republishing the saline water wedge. A comparison of the effectiveness of different hydraulic barriers system to

control saline water intrusion in coastal areas is provided by Ebeling et al. (2019). Other seawater control method was suggested by Strack et al. (2016), who showed that a reduction in the hydraulic conductivity in the upper part of a coastal aquifer would lead to a substantial reduction in the saltwater intrusion length and presented valuable analytical expressions based on the work of Strack and Ausk (2015). It is nonetheless important to note that the study of Strack et al. (2016) focused solely on steady-state conditions and considered a single thickness of the top layer throughout their investigation. In addition, the effect of sea level fluctuations on the performance of the countermeasure was not within the scope of their investigation.

The main purpose of this study is to assess systematically and quantitatively the impact of a top low-permeability (TLK) layer on the saltwater wedge response to water level changes under controlled laboratory setting. In addition to providing an insight on saltwater dynamics in semi-confined coastal aquifers, this study also investigates the worthiness of reducing artificially the upper portion of the aquifer to control SWI (Strack et al., 2016). For the first time, the impact of a TLK layer on the saltwater wedge response to freshwater and saltwater level fluctuations was quantitatively analysed, under both steady state and transient conditions. In addition, three scenarios were investigated whereby the TLK layer thickness was gradually increased to 20%, 33%,

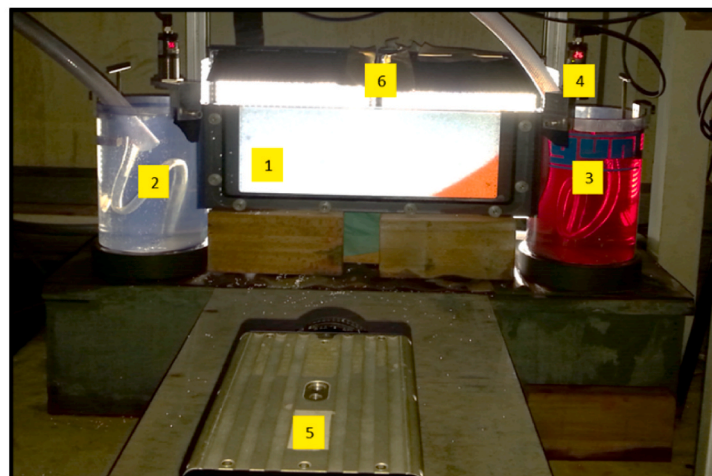
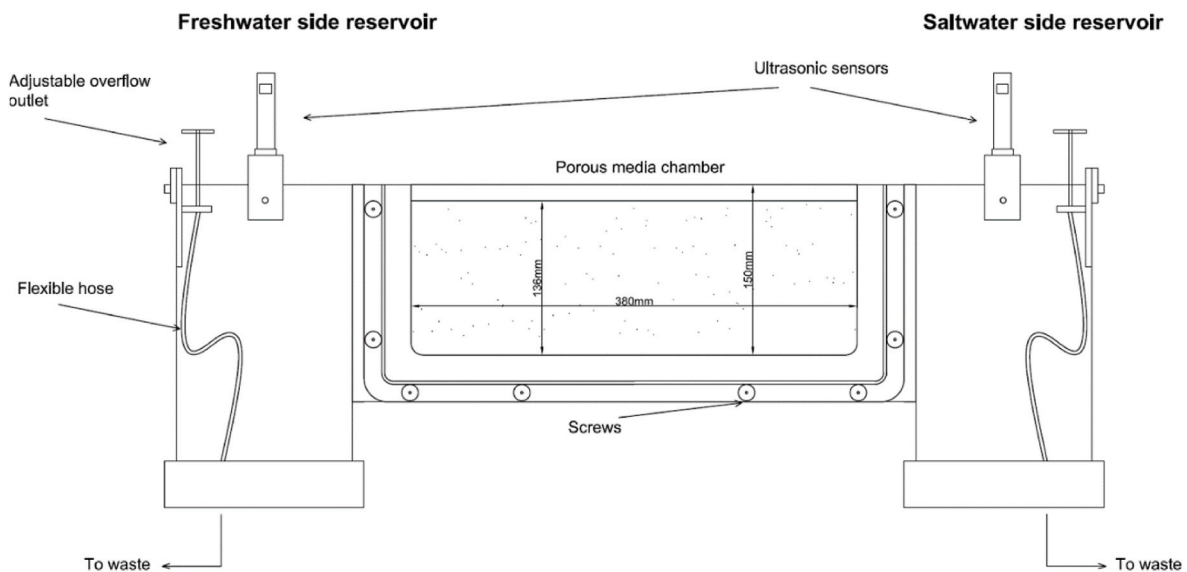


Fig. 1. Schematic diagram (top) and a photograph (bottom) of the experimental Setup; 1) porous media chamber; 2) freshwater reservoir; 3) saltwater reservoir; 4) ultrasonic sensors; 5) high speed camera; 6) LED lights.

and 50% of the total aquifer thickness, respectively. Experimental automated image analysis technique was implemented to enable the accurate measurement of the saltwater wedge length with high spatial and temporal resolutions. Numerical modelling was used for the purpose of validation and to conduct both laboratory-scale and field scale simulations in order to examine how the main design and hydrogeological parameters impact the ability of the TLK layer to reduce SWI in coastal aquifers.

2. Materials and methods

2.1. Experimental methods

The experimental methodology was described in detail in other studies (e.g., [Robinson et al., 2015, 2016](#); [Abdoulhalik and Ahmed, 2018](#)), so it will be described briefly herein. A laboratory flow tank of dimension $0.38 \text{ m} \times 0.15 \text{ m} \times 0.01 \text{ m}$ was used for the experiments ([Fig. 1](#)). The tank was composed of three main parts, namely a central chamber to simulate the porous media and two side reservoirs at either side to impose head boundary conditions. Two fine mesh acrylic screens separated the central chamber from the side reservoirs. Clear glass beads were used to simulate the porous media. These were siphoned into the central chamber under saturated conditions to avoid risks of air entrapment.

Two different bead sizes were used: $780 \mu\text{m}$ beads for the upper layer and $1325 \mu\text{m}$ beads for the bottom layer and also for the homogeneous case used here as a benchmark. The hydraulic conductivity of each of these beads was estimated using in situ measurement within the experimental flow tank. Several hydraulic gradients were applied to the system, and the corresponding volumetric freshwater discharge was measured ([Abdoulhalik et al., 2017](#); [Abdoulhalik and Ahmed, 2017a, b](#)). The values of the average conductivity were estimated at 36 cm/min and 108 cm/min for the beads $780 \mu\text{m}$ and $1325 \mu\text{m}$, respectively. Three scenarios were investigated, where the ratio of the TLK layer thickness to the total aquifer thickness was set to 20%, 33%, and 50%. These scenarios are designated hereafter as cases 0.2H, 0.33H, and 0.5H, respectively.

Freshwater and saltwater were supplied to the system from the left and right-side reservoirs, respectively. The saltwater for all experiments was sourced from a 200 L saltwater solution that was prepared prior to the experiments by dissolving commercial salt into cold tap water at a concentration of 36.16 g/L such that to obtain a saltwater density of 1025 kg/m^3 . To distinguish the saltwater from the freshwater, the saltwater solution was dyed using red food colour at a concentration of 0.15 g/L ([Robinson et al., 2015](#)).

A fixed head of 12.97 cm was set on the saltwater reservoir, and an excess amount of saltwater was constantly supplied to flush out any freshwater floating at the surface until the density measurement became stable. Ultrasonic sensors (Microsonic - mic+25/DIU/TC) were used to continuously monitor the head values. Two head differences (dh) were examined, namely $dh = 3.6 \text{ mm}$ and 6 mm between the freshwater and saltwater boundaries. This is equivalent to hydraulic gradients of 0.94% and 1.58% respectively. The hydraulic gradients used here are consistent with previous laboratory studies using similar setup ([Robinson et al., 2015, 2016](#); [Chang and Clement, 2012](#)) and within the range of hydraulic gradient measured at some field sites (e.g., [Ferguson and Gleesson, 2012](#)). The set of experiments involving freshwater head variations with constant saltwater boundary are referred to as FW in the forthcoming figures. The sets of experiments where the saltwater level was changed while the freshwater boundary was held constant are referred to as SW. In this latter set of experiments, the freshwater boundary was held constant at $h = 13.57 \text{ mm}$ while the saltwater head boundary was increased up from 12.97 to 13.21 cm .

Two LED lights were placed behind the setup, and a light diffuser was fixed to the back of the tank to homogenise the light throughout the porous media. A correlation between the intensity of the light

transmitted through the porous media and the saltwater concentration was established through a calibration procedure as described in detail in [Robinson et al. \(2015\)](#).

2.2. Numerical methods

The SEAWAT code ([Guo and Langevin, 2002](#)) was adopted in this study to assess the validity of the experimental results and to further examine the impact of the existence of a TLK layer on saltwater intrusion length in realistic coastal aquifer conditions. The SEAWAT code has been widely used for saltwater intrusion problems involving sandbox experiments ([Chang et al., 2011](#); [Abdoulhalik et al., 2017](#); [Abdoulhalik and Ahmed, 2017a, b](#)).

For the small-scale simulations, a rectangular model $38 \times 14 \text{ cm}$ was built to represent the porous media. The domain was uniformly discretized using size mesh of 0.2 cm . The dispersivity values were estimated via trial-and-error process such that the longitudinal and transverse dispersivity were estimated at 0.1 cm and 0.05 cm . These dispersivity values remain within the range suggested by [Abarca and Clement \(2009\)](#) for a similar range of bead size. The spatial discretization and dispersivity values provided numerical stability by satisfying the grid Peclet number criterion. The molecular diffusion was neglected in this study ([Riva et al., 2015](#)). A constant head was set at the coastal boundary ($C = 36.16 \text{ g/L}$), and the variable boundary head was set at the inland freshwater boundary ($C = 0 \text{ g/L}$). Like the experiment, the simulation time was set at $t = 50 \text{ min}$ for each head difference tested, with a time step of 30 s .

For the field-scale simulations, the dimensions of the model were $400 \text{ m} \times 1 \text{ m} \times 20 \text{ m}$ such that x was the horizontal length of the aquifer perpendicular to the beach, z was the thickness of the aquifer, and y was the width of the aquifer along the coastline. The seawater intrusion process was therefore depicted within the (x, z) plan. The grid dimensions were $2 \text{ m} \times 1 \text{ m} \times 1 \text{ m}$ in the x , y , and z directions, respectively. The longitudinal dispersivity was set to 1 m , with a transversal dispersivity of 0.1 m . The saltwater density was set to 1025 kg/m^3 , with the seawater head boundary fixed at 19.2 m . A variable head was set at the freshwater boundary, which was gradually decreased from 20 m to 19.4 m with a constant step of 0.2 m , yielding four different head differences, specifically $dh = 0.8, 0.6, 0.4$ and 0.2 m . Each stress period was run for 5000 days such that to ensure the system reached steady-state condition.

3. Results and discussion

The experimental data of the saltwater toe length of the investigated cases are shown in [Table 1](#). The results show that the TLK layer induces shorter intrusion lengths in both freshwater and saltwater head change scenarios. The extent of the saltwater intrusion length was further reduced as the thickness of the TLK increased. This is because the freshwater is forced to flow mainly through the bottom layer due to the lower permeability of the top layer, thereby inducing higher repulsion forces to the saltwater wedge. This observation agrees with the results presented in [Strack et al. \(2016\)](#). The toe length values in the sea level rise scenario are greater compared to the freshwater head drops, especially for $dh = 3.6 \text{ mm}$, due to the higher larger saturated thickness in

Table 1
Experimental toe length results in cm.

Head change	Cases	Homogeneous	0.2H	0.33H	0.5H
Freshwater variations	$dh = 3.6 \text{ mm}$	25.3	23	20.8	19.3
	$dh = 6 \text{ mm}$	8.6	8.2	6.6	5.9
Saltwater variations	$dh = 3.6 \text{ mm}$	28.2	24.3	23.5	19.5
	$dh = 6 \text{ mm}$	8.4	8.3	6.6	6.3

the former scenario compared to the latter.

Interestingly, the toe length decreased in a linear fashion with increasing the ratio W_{top}/H (Fig. 2). This finding provides a relatively convenient way to make an approximate estimate of the saltwater intrusion length reduction achievable by lowering the permeability of the upper part of a coastal aquifer. In coastal groundwater systems with a homogeneous isotropic aquifer, the amount of the reduction of the intrusion length could be reasonably well predicted by developing a linear relationship relating the toe length to the ratio W_{top}/H . Once the regression coefficients of the equation are derived, the relationship could be used to estimate the achievable amount of reduction of the saltwater length for other ratios W_{top}/H .

The numerical model SEAWAT was used for the numerical simulations of the experimental cases. The initial condition of the model represented an aquifer with fully freshwater. The transient progression of the saltwater wedge was reproduced over two stress periods. In the first, saline water was allowed to enter the model domain and reach a first steady-state condition following the application of heads of 13.33 cm and 12.97 cm ($d_h = 3.6$ mm), at the freshwater ($C = 0$ g/L) and saltwater boundary ($C = 36.16$ g/L), respectively, like the physical experiments. In the following stress period, the freshwater head was successively increased to 13.57 cm to establish $d_h = 6$ mm, to force the retreat of the saltwater wedge towards the seawater boundary. Only the scenario involving inland freshwater variations was simulated.

The transient experimental data of the receding saltwater wedge following the rise of the freshwater head back to $d_h = 6$ mm along with the associated numerical results are presented in Fig. 3. In overall, the numerical model was able to accurately predict the transient motion of the receding wedge in all the different cases. Some mismatch could be observed in the early stage of the retreat, where the toe motion predicted by the numerical was slightly faster than in the physical model. This trend has been observed in previous similar studies (Chang and Clement, 2012; Robinson et al., 2016). Both experimental and numerical results show that the TLK layer induced a faster receding wedge than in the homogeneous case, which shows that lowering the permeability of the upper part of the aquifer causes faster saltwater removal process. Also, the numerical model shows perfect linearity in the relationship between the steady-state toe length and the ratio of the TLK layer thickness over the aquifer height, which agrees with the experimental observations (Fig. 4).

4. Sensitivity analysis

Further numerical simulations were conducted to explore the sensitivity of the toe length to the influential parameters such as the upper layer hydraulic conductivity, porosity and dispersivity of the main aquifer, and freshwater/seawater density contrast.

A further decrement of the toe length occurred following the rise of the ratio K/K_{top} (Fig. 5). As K/K_{top} was increased from 1 to 9, the toe length was reduced by about 7% and 22% for $W_{top} = 0.2H$ and $W_{top} =$

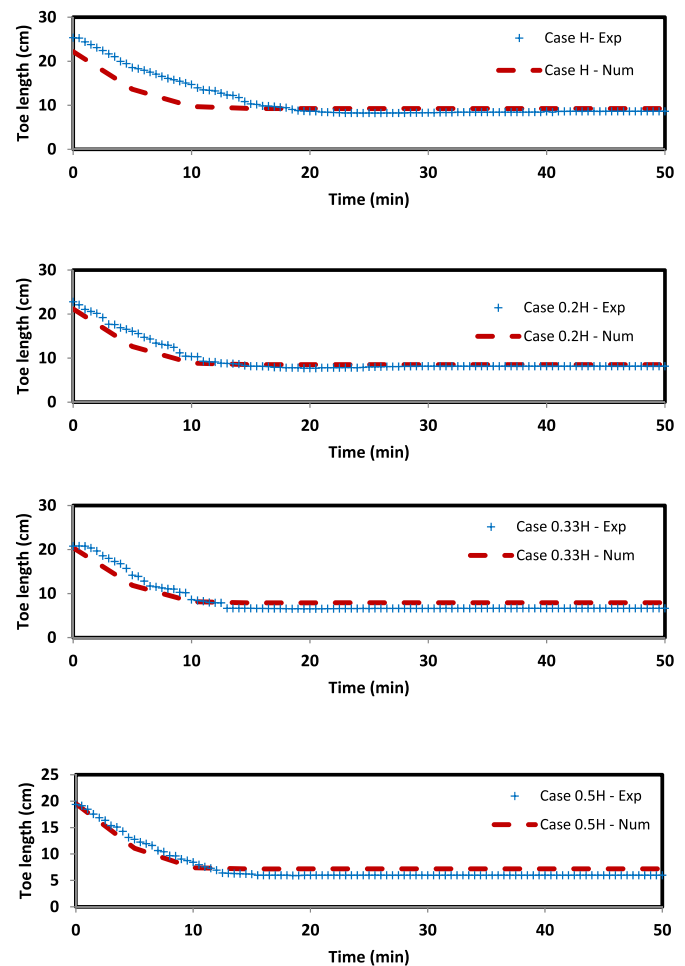


Fig. 3. Comparison between experimental and numerical transient toe length data.

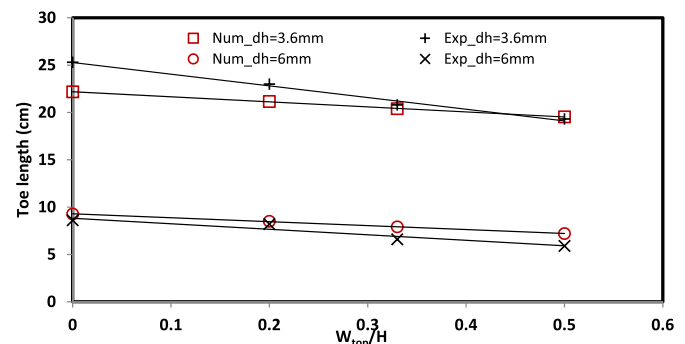


Fig. 4. Numerical and experimental toe length against the ratio of the TLK layer thickness and the aquifer height.

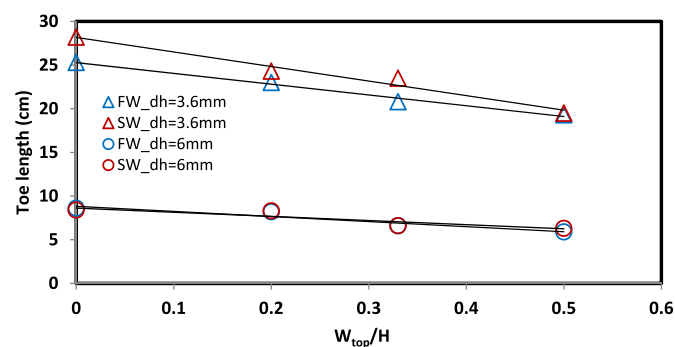


Fig. 2. Experimental toe length against the ratio of the top layer thickness and the aquifer thickness.

0.5H, respectively. In other words, for equivalent reduction of the upper layer permeability, the reduction of the toe length would be substantially greater as the thickness of the upper layer is larger. The results nonetheless show that regardless of the permeability reduction, this method yields relatively little reduction of the saline water intrusion length if the upper layer thickness is inferior or equal to a fifth of the total aquifer thickness. The results also show that reasonable reduction could be achieved in case where the permeability of half the aquifer thickness is lowered, which seems impractical and expensive in real-world problems, where the cost of implementing such method would highly increase with increasing top layer thickness and the land size that

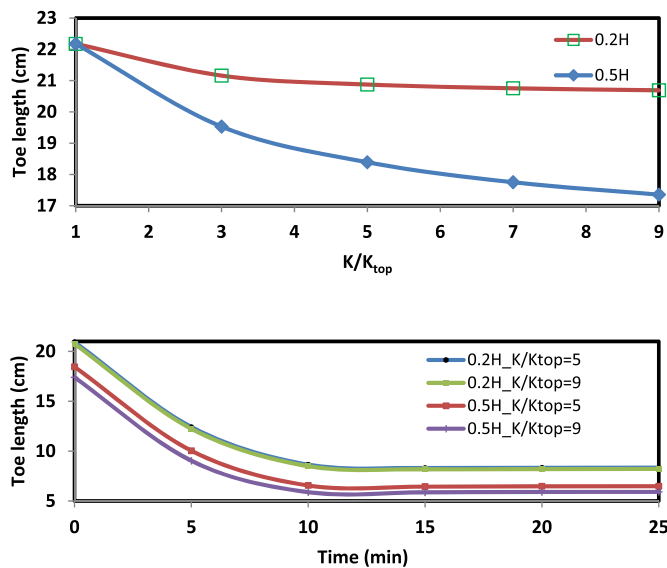


Fig. 5. Sensitivity of the TLK performance to hydraulic conductivity a) Change of TL with permeability ratio, and b) transient TL at retreat for different permeability ratios.

needs to be covered.

The transient data of the saltwater retreat presented in Fig. 5 show that the receding rate of the saltwater retreat was little sensitive to the variations of the ratio K/K_{top} . In other words, decreasing the permeability of the top layer induced little effects on the receding rate of the saltwater wedge, regardless of the permeability of the top layer. This is clearer in the case where the TLK layer counted for a fifth of the aquifer thickness, whereby the changes in the top layer permeability did not introduce any effect on the rate of the saltwater wedge retreat following the freshwater boundary head variation.

The impact of the aquifer dispersivity on the toe length reduction caused by the TLK layer is shown in Fig. 6. The results show that the extent of the toe length decreases with increasing dispersivity of the main aquifer. For $W_{top} = 0.2H$, the toe length extended up to 24 and 19.7 cm as dispersivity was increased from 0.01 cm to 0.2 cm,

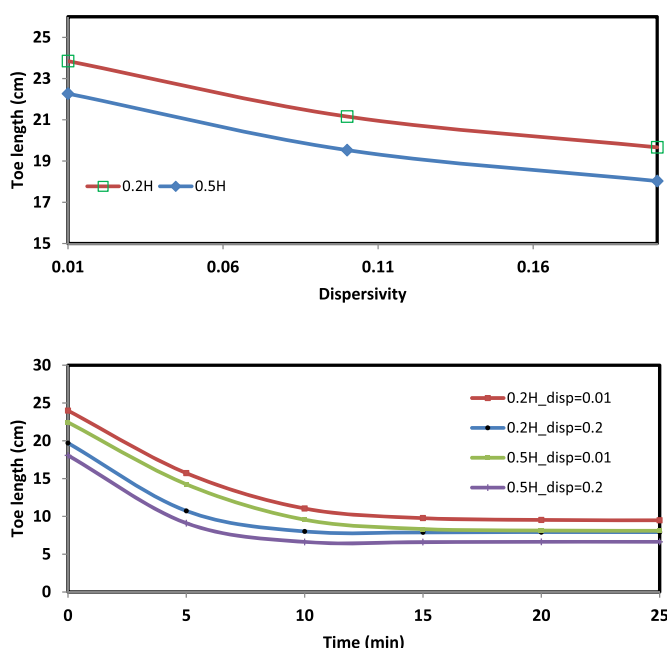


Fig. 6. Sensitivity of the TLK performance to dispersivity.

respectively. For $W_{top} = 0.5H$, the toe length reduced from 22.3 cm to 18 cm (i.e., about 20% reduction), as the dispersivity increased from 0.01 cm to 0.2 cm, respectively.

In other words, for the same increment of the dispersivity from 0.01 cm to 0.2 cm, the reduction achieved by the TLK layer was about 18% and 20% for $W_{top} = 0.2H$ and $W_{top} = 0.5H$, respectively. The receding rate of the saltwater wedge appeared relatively similar and has approximately the same sensitivity to the dispersivity incremental increase for different thicknesses of the TLK layer. The transient data show that the rate of saltwater retreat was slightly faster for greater dispersivity in both cases, leading to the steady state reached slightly sooner.

Under conditions like those adopted in the above analyses for W_{top} of 0.2H and 0.5H, the impact of the saltwater density on the toe length was investigated and the results are shown in Fig. 7. As expected, the higher the density, the larger the toe length. The toe length was 14.1 cm and 30.7 cm for the $W_{top} = 0.2H$; and 12.5 cm and 29.7 cm for $W_{top} = 0.5H$, for a saltwater density of 1020 kg/m³ and 1030 kg/m³, respectively. The reduction of the toe length shows more sensitivity for lower density values. The retreat was slightly affected by the increase in density. The saltwater wedge reached steady state faster for the lower density scenario than the high-density scenario. This may be because when the saltwater density is smaller, it is easier for the freshwater flow to push back the saltwater wedge, as the buoyancy force is lowered.

The effect of the porosity on the reduction of toe length was explored over the range 0.2–0.5 and the results show that the rate of toe length reduction following the implementation of the TLK layer exhibits no sensitivity to the porosity of the aquifer, neither in steady state nor in transient condition (Figure is not shown for brevity).

5. Field scale modelling

A field-scale aquifer model was developed to further explore the effectiveness of TLK layer in more realistic coastal aquifer settings. The hydraulic conductivity of the homogeneous aquifer was set to 5 m/day. In all the simulations, K_{top} was set to 1 m/day, such that the permeability of the low top layer accounted for a fifth of the aquifer permeability. To examine the effect of the thickness of the TLK layer on the seawater intrusion reduction, four values of W_{top} were tested such that $W_{top} = 0, 0.25H, 0.5H$ and $0.75H$. Note that the top layer thickness $W_{top} = 0.75H$ was only adopted for the sake of the analysis, as lowering such large part of the aquifer thickness is not practical in real-world conditions. The

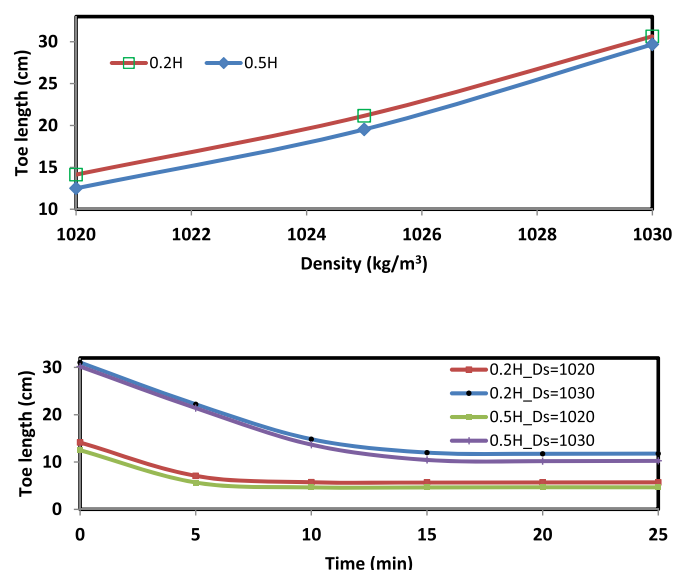


Fig. 7. Sensitivity of the TLK performance to saltwater density.

scenario where $W_{top} = 0$ corresponded to the homogeneous scenario, which was taken as the base case in the calculation of the toe length reduction caused by the implementation of the TLK layer.

In the homogeneous case, the resulting saltwater wedge toe length values were 101.4, 143.2, 191.2, and 250.5 m for head differences of 0.8 m, 0.6 m, 0.4 m, and 0.2 m respectively. Fig. 8 shows the toe length response to increasing TLK layer thickness. Again, the results show that the toe length decreases linearly with increasing top layer thickness, in agreement with the experimental observations. At the initial head difference ($dh = 0.8$ m), the results show that the toe length was reduced by 11.3, 24.2 and 31.4 m, for $W_{top} = 0.25H$, $0.5H$ and $0.75H$, respectively. At the final head difference ($dh = 0.2$ m), the toe length was reduced by 20.8, 44.2 and 56.4 m for $W_{top} = 0.25H$, $0.5H$ and $0.75H$, respectively. Hence, for $W_{top} = 0.25H$, $0.5H$ and $0.75H$, the TLK layer achieved a SWI reduction of 11%, 24% and 31% at $dh = 0.8$ m, respectively, and 8%, 18%, and 23% at $dh = 0.2$ m, respectively. Hence, the performance of the TLK layer was reduced by 3%, 6% and 8% from the initial to the final hydraulic gradient, which therefore demonstrates that the impact of the TLK layer on SWI weakens as the hydraulic gradient decreases. These field scale results agree with the laboratory experiments observations that showed greater seawater toe length reduction at larger hydraulic gradient for different thicknesses of the TLK layer.

The implementation of a TLK layer with a thickness $W_{top} = 0.25H$ yielded insignificant reduction values for all the tested hydraulic gradients, in agreement with the experimental observations (Fig. 8). At that thickness, the TLK layer achieved nearly the same toe length reduction

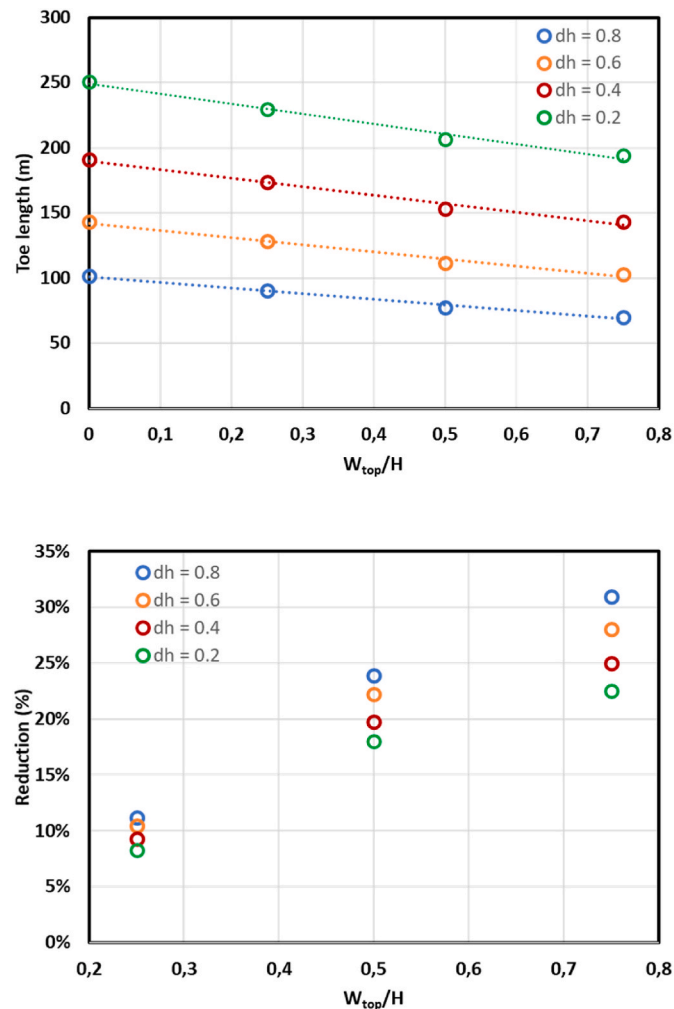


Fig. 8. Impact of the top layer thickness on the saltwater intrusion length (top) and the associated percentage of reduction (bottom).

for all hydraulic gradients, while more disparities could be observed between the reduction values as the top layer thickness was increased. The results also demonstrate that the maximum toe length reduction achieved by the TLK layer was 31%, which occurred in the case where $W_{top} = 0.75H$. In other words, the data suggest that lowering the permeability of up to three fourths of the aquifer thickness induced a reduction of the toe length by nearly a third of its original length in a homogeneous aquifer scenario.

This investigation provided a transient and steady-state analysis of SWI in heterogeneous settings with the aim of providing an insight on the impact of an overlaying low-K layer on SWI intrusion length. The outcomes of this study show for the first time the existence of a linear relationship between the toe length and the width of the overlying low K layer, both in small-scale (physical and numerical) and field-scale models for various sets of hydrogeological parameters. Specifically, the findings derived under laboratory conditions were validated by the small-scale numerical model and further confirmed in the field-scale aquifer model, where the existence of a linear correlation between the toe length and the width of the TLK was also evidenced in more realistic scenarios for various sets of hydrogeological parameters.

The findings derived in this study are not only important from a water resources management perspective as they evidence the relatively low effectiveness of reducing artificially the top portion of a coastal aquifer to control seawater intrusion, regardless of the boundary water level variations and hydrogeological conditions. Simultaneously, the results also demonstrate quantitatively the influence of an overlaying low permeability layer on the extent of saltwater wedges in coastal aquifers submitted to periodic changes in the hydrological stresses.

6. Summary and results

The impact of a top low-permeability (TLK) layer on seawater intrusion was quantitatively analysed using physical experiments and numerical simulations. Four cases were investigated, including a homogeneous case and three cases where the top layer thickness was gradually increased such that it equalled to $0.2H$, $0.33H$ and $0.5H$, respectively, with H being the total aquifer thickness. The numerical model SEAWAT was used for the purpose of validation. Additional simulations were thereafter conducted using the validated numerical model to explore how the main design and hydrogeological parameters impact the ability of the TLK layer to reduce SWI. For the sake of completeness, the influence of these key parameters on the effectiveness of the TLK layer was also examined in a field-scale numerical model. The main findings of this investigation can be summarised as follows:

- Reducing the permeability of only 20% of the total aquifer thickness induced insignificant reduction of the saltwater wedge length. A noticeable reduction could only be achieved when the TLK layer thickness was about 50% of the total aquifer thickness, albeit lowering the permeability of half the aquifer thickness would most likely be impractical in real world problems.
- Experimental and numerical simulations results (laboratory and field-scale) provide strong evidence that the saltwater intrusion length decreases linearly with increasing thickness of the TLK layer.
- Both experimental and numerical results show that the bi-layered aquifer with top low permeability layer induced a faster receding process than a homogeneous aquifer, which demonstrate that lowering the permeability of the upper part of the aquifer causes faster removal of saline water from the aquifer.
- For the aquifer setting considered herein, the sensitivity analysis shows that further reduction of the top layer permeability shortens the toe length only when the TLK layer equals or exceeds half of the aquifer thickness. The sensitivity analysis also show that in the presence of the TLK, the toe length was reduced by about 20% as the aquifer dispersivity increased from 0.01 to 0.2 cm. The sensitivity

analyses also show that the reduction of the toe length exhibited more sensitivity in lower saltwater density scenarios.

- The field-scale modelling results demonstrate that the performance of the TLK layer weakens noticeably as the hydraulic gradient decreases. The TLK layer achieved a maximum saltwater wedge reduction of 31% in the case where its thickness was equivalent to 75% of the total saturated thickness. In other words, lowering the permeability of three fourths of the aquifer thickness could only induce a toe length reduction by nearly a third of its original length. Hence, these results seriously question the effectiveness and practicality of reducing artificially the upper portion the aquifer to control for seawater intrusion in coastal regions.

Future investigations could explore how the effect of aquifer bed slope and/or the third dimension (along the coastline) may impact saltwater intrusion dynamics in the presence of a TLK layer. Additionally, examining whether a TLK layer combined with hydraulic barriers would enhance the reduction of SWI would also be worthy of further analyses. These control methods could be assessed using the GLADIT method (e.g., Kazakis et al., 2019), which may be included as a new parameter.

Credit author statement

Antoifi Abdoulhalik: Conceptualization, Methodology, experimental work, writing draft manuscript. Ashraf Ahmed: Conceptualization, numerical modelling, editing, Supervision. A Abdelgawad: Numerical modelling, Software. G Hamill: Editing, Supervision.

Declaration of competing interest

The authors declare that they have no known competing financial interests or personal relationships that could have appeared to influence the work reported in this paper.

References

- Abarca, E., Clement, T.P., 2009. A novel approach for characterizing the mixing zone of a saltwater wedge. *Geophys. Res. Lett.* 36 (6), L06402.
- Abdoulhalik, A., Ahmed, A.A., 2017a. How does layered heterogeneity affect the ability of subsurface dams to clean up coastal aquifers contaminated with seawater intrusion? *J. Hydrol.* 553, 708–721. <https://doi.org/10.1016/j.jhydrol.2017.08.044>.
- Abdoulhalik, A., Ahmed, A.A., 2017b. The effectiveness of cutoff walls to control saltwater intrusion in multi-layered coastal aquifers: experimental and numerical study. *J. Environ. Manag.* 199, 62–73. <https://doi.org/10.1016/j.jenvman.2017.05.040>.
- Abdoulhalik, A., Ahmed, A.A., 2018. Transience of seawater intrusion and retreat in response to incremental water-level variations. *Hydrol. Process.* 32 (17), 2721–2733.
- Abdoulhalik, Antoifi, Ahmed, Ashraf, Hamill, G., 2017. A new physical barrier system for seawater intrusion control. *J. Hydrol.* 549, 416–427.
- Armanuos, A.M., Ibrahim, M.G., Mahmood, W.E., Takemura, J., Yoshimura, C., 2019. Analysing the combined effect of barrier wall and freshwater injection countermeasures on controlling saltwater intrusion in unconfined coastal aquifer systems. *Water Resour. Manag.* 33 (4), 1265–1280.
- Botero-Acosta, A., Donado, L.D., 2015. Laboratory scale simulation of hydraulic barriers to seawater intrusion in confined coastal aquifers considering the effects of stratification. *Procedia Environ. Sci.* 25, 36–43.
- Chang, S.W., Clement, T.P., 2012. Experimental and numerical investigation of saltwater intrusion dynamics in flux-controlled groundwater systems. *Water Resour. Res.* 48 (9), W09527.
- Chang, S.W., Clement, T.P., Simpson, M.J., Lee, K., 2011. Does sea-level rise have an impact on saltwater intrusion. *Adv. Water Resour.* 43 (10), 1283–1291.
- Chang, Q., Zheng, T., Zheng, X., Zhang, B., Sun, Q., Walther, M., 2019. Effect of subsurface dams on saltwater intrusion and fresh groundwater discharge. *J. Hydrol.* 576, 508–519.
- Ebeling, P., Händel, F., Walther, M., 2019. Potential of mixed hydraulic barriers to remediate seawater intrusion. *Sci. Total Environ.* 693, 133478.
- Ferguson, G., Gleeson, T., 2012. Vulnerability of coastal aquifers to groundwater use and climate change. *Nat. Clim. Change* 2, 342–345.
- Guo, W., Langevin, C.D., 2002. User's Guide to SEAWAT; a Computer Program for Simulation of Three-Dimensional Variable-Density Ground-Water Flow.
- Kazakis, N., Busico, G., Colombani, N., Mastrocicco, M., Pavlou, A., Voudouris, K., 2019. GALDIT-SUSI a modified method to account for surface water bodies in the assessment of aquifer vulnerability to seawater intrusion. *J. Environ. Manag.* 235, 257–265.
- Luyun Jr., R., Momii, K., Nakagawa, K., 2009. Laboratory-scale saltwater behavior due to subsurface cutoff wall. *J. Hydrol.* 377, 227–236.
- Pool, M., Carrera, J., 2010. Dynamics of negative hydraulic barriers to prevent seawater intrusion. *Hydrogeol. J.* 18 (1), 95–105.
- Riva, M., Guadagnini, A., Dell'Oca, A., 2015. Probabilistic assessment of seawater intrusion under multiple sources of uncertainty. *Adv. Water Resour.* 75, 93–104.
- Robinson, G., Ahmed, A.A., Hamill, G.A., 2016. Experimental saltwater intrusion in coastal aquifers using automated image analysis: applications to homogeneous aquifers. *J. Hydrol.* 538, 304–313. <https://doi.org/10.1016/j.jhydrol.2016.04.017>.
- Robinson, G., Hamill, G.A., Ahmed, A.A., 2015. Automated image analysis for experimental investigations of salt water intrusion in coastal aquifers. *J. Hydrol.* 530, 350–360. <https://doi.org/10.1016/j.jhydrol.2015.09.046>.
- Strack, O.D.L., Ausk, B.K., 2015. A formulation for vertically integrated groundwater flow in a stratified coastal aquifer. *Water Resour. Res.* 51 (8), 6756–6775.
- Strack, O.D.L., Stoeckl, L., Damm, K., Houben, G., Ausk, B.K., de Lange, W.J., 2016. Reduction of saltwater intrusion by modifying hydraulic conductivity. *Water Resour. Res.* 52, 6978–6988.